INWARD RECTIFIER K^+-CHANNEL KINETICS FROM ANALYSIS OF THE COMPLEX CONDUCTANCE OF *APLYSIA* NEURONAL MEMBRANE

HATSUO HAYASHI AND HARVEY M. FISHMAN
Department of Physiology and Biophysics, University of Texas Medical Branch, Galveston, Texas 77550

ABSTRACT Conduction in inward rectifier, K^+-channels in *Aplysia* neuron and Ba^{++} blockade of these channels were studied by rapid measurement of the membrane complex admittance in the frequency range 0.05 to 200 Hz during voltage clamps to membrane potentials in the range −90 to −40 mV. Complex ionic conductances of K^+ and Cl^- rectifiers were extracted from complex admittances of other membrane conduction processes and capacitance by vector subtraction of the membrane complex admittance during suppressed inward K^+ current (near zero-mean current and in zero $[K^+]_0$) from complex admittances determined at other $[K^+]_0$ and membrane potentials. The contribution of the K^+ rectifier to the admittance is distinguishable in the frequency domain above 1 Hz from the contribution of the Cl^- rectifier, which is only apparent at frequencies <0.1 Hz. The voltage dependence (−90 to −40 mV) of the chord conductance (0.2 to 0.05 μS) and the relaxation time (4–8 ms) of K^+ rectifier channels at $[K^+]_0$ = 40 mM were determined by curve fits of admittance data by a membrane admittance model based on the linearized Hodgkin-Huxley equations. The conductance of inward rectifier, K^+ channels at a membrane potential of −80 mV had a square-root dependence on external K^+ concentration, and the relaxation time increased from 2 to 7.5 ms for $[K^+]_0$ = 20 and 100 mM, respectively. The complex conductance of the inward K^+ rectifier, affected by Ba^{++}, was obtained by complex vector subtraction of the membrane admittance during blockage of inward rectifier, K^+ channels (at −35 mV and $[Ba^{++}]_0$ = 5 mM) from admittances determined at −80 mV and at other Ba^{++} concentrations. The relaxaton time of the blockade process decreased with increases in Ba^{++} concentration. An open-closed channel state model produces the inductive-like kinetic behavior in the complex conductance of inward rectifier, K^+ channels and the addition of a blocked channel state accounts for the capacitive-like kinetic behavior of the Ba^{++} blockade process.

1. INTRODUCTION

In addition to the classical Na^+ and K^+ currents found in the squid giant axon, neuronal membrane exhibits complicated electrical phenomena as a result of the following voltage sensitive currents: a transient Ca^{++} current (Geduldig and Gruener, 1970), a slowly inactivating Ca^{++} current (Eckert and Lux, 1976), a fast transient K^+ current (Hagiwara et al., 1961), an "anomalously" rectifying K^+ current (Kandel and Tauc, 1964), a slow K^+ current (Brodwick and Junge, 1972), and a Ca^{++}-activated K^+ current (Meech and Standen, 1975). The anomalous rectifier is the only one of these proceses that is activated at membrane voltages more hyperpolarized than the potassium equilibrium potential (E_K). Noble (1979) suggested that the functional role of the inward rectifier in heart muscle is to keep the resting potential of the cell near E_K without producing significant K^+ efflux during an action potential.

After Katz (1949) initially found rectification of the inward K^+ current in frog twitch muscle fibers, this process was studied in neurons of *Helix* (Kandel and Tauc, 1964; Kandel and Tauc, 1966), *Anisodoris* (Marmor, 1971), muscle membranes (Hutter and Noble, 1960; Reuben and Gainer, 1962; Nakajima et al., 1962; Adrian and Freygang, 1962; Adrian et al., 1970; Leech and Stanfield, 1981; Hestrin, 1981), retinal rods (Werblin, 1979), macrophages (Gallin, 1981), cut spinal motorneurons (Nelson and Frank, 1967), and in egg cells (Hagiwara and Takahashi, 1974; Ohmori, 1980; Gunning, 1983; Gunning, 1984). Wide occurrence of rectification of inward K^+ current, especially in cells that exhibit complicated behavior, suggests that it is important.

The dependence of the relaxation time of the inward K^+ rectifier on membrane potential and K^+ concentration have been investigated in muscle membranes (Adrian et al., 1970; Leech and Stanfield, 1981; Hestrin, 1981) and marine polychaete eggs (Gunning, 1983; Gunning, 1984) by analysis of step voltage-clamp current responses.

Dr. Hayashi's present address is Department of Computer Science and Electronics, Kyushu Institute of Technology, Iizuka, Fukuoka 820, Japan

Recent patch clamp studies of inward rectifier channels in heart cells showed that the open-channel conductance is ohmic and that the steady-state rectification is due to the gating kinetics of channel conduction at membrane voltages depolarized from E_K and by a voltage-induced blockage of the channel by cytoplasmic-side Mg^{++} at higher than physiological external K^+ concentrations (Matsuda et al., 1987; Vandenberg, 1987). In molluscan neurons, anomalous rectification has been observed in the current-voltage relationship; however, these results have not been reported and the relaxation time of the rectifier channel has not been determined.

Here, the electrical properties and kinetics of inward rectifier, K^+ channels in *Aplysia* neurons were studied by analysis of rapid admittance determinations, made during voltage clamp steps (Fishman et al., 1981), because of the advantages of this method over analysis of step voltage-clamp transient currents. Both Cl^- and K^+ participated as carriers of the inward current in the rectification process and, below 100 Hz, both ion conductances appeared as distinct and separable components in the frequency domain (different relaxation times). The inward rectifier K^+ conductance increased and its relaxation time decreased with hyperpolarization. The conductance was proportional to the square root of external K^+ concentration and the relaxation time increased with increasing K^+ concentration. An external Ba^{++} concentration of 5 mM was found to block inward rectifier, K^+ channels and the blocking process produced a capacitive-like kinetic behavior in the admittance, which could be described adequately by a two-state Markov model. A preliminary report of this work has appeared (Hayashi and Fishman, 1986).

2. METHODS

2-1. Experiments

Neurons in the abdominal ganglion of *Aplysia californica*, obtained from Alacrity Marine Biological Services Co., Redondo Beach, California, were used in these experiments. An abdominal ganglion was isolated from the body of *Aplysia* and the ganglion was fixed in pool A of a measuring chamber (Fig. 1) by pinning five nerves from the ganglion. The ganglion was treated in artificial sea water with 0.2% trypsin (type XI: Sigma Chemical Co., St. Louis, MO) for 8 min at 23–24°C to soften the connective tissue capsule. Then the capsule was removed with tweezers and a small razor-blade knife in order to expose the neurons. The size of the neurons that were used in these experiments was 105–225 μm in diameter.

Fig. 1 shows a schematic diagram of the voltage clamp system employed in admittance measurements (0.05–1,000 Hz). Two microelectrodes were used: one for voltage sensing and the other for current injection. The resistance of each electrode, filled with 3 M KCl, was 4–5 MΩ. High frequency roll-off in the voltage of the input voltage stage was reduced by driving a shield which surrounded both the voltage-sensitive microelectrode and the input stage with a buffered replica of the sensed voltage. Thus the current flow, at high frequency, through stray capacitance-to-ground was reduced to an extent that the frequency response of the current was flat out to 1 kHz. Current through the preparation was measured with a virtual-ground operational amplifier, which was connected to a Ag-AgCl pellet in the bath and ground. The solution was dropped into pool B through a needle in order to reduce stray capacitance

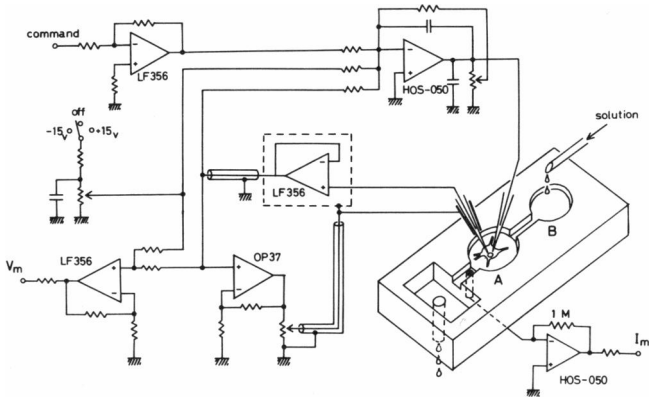

FIGURE 1 Schematic diagram of the voltage-clamp measurement system and preparation chamber. See text for details.

by disconnecting the chamber from the solution bottles. The neurons were continuously perfused with fresh solution; the flow rate was ~0.5 ml/min.

The external solutions used in these experiments are listed in Table I. In solutions I and II, Na^+ was replaced by N-methyl-d-glucamine to suppress the Na^+ current. The Ca^{++} current was also suppressed by 1 mM Ni. K^+ in solution I was exchanged with isosmolar N-methyl-d-glucamine when the K^+ concentration dependence of the inward K^+ rectifier was observed. Ba^{++} was used as a blocker. When the effect of Ba^{++} on the rectifier was investigated Mg^{++} in solution II was replaced by isosmolar Ba^{++}.

After replacing artificial sea water with K^+-free solution I, the neurons were left to equilibrate in the solution for at least 1 h in order to deplete Na^+ and K^+ from the clefts of the cell body and to suppress Ca^{++} current. Then microelectrodes were inserted into the cell body. A steady-state current-voltage curve and an admittance function were obtained by measuring steady state currents 10 s after application of long-duration step voltage clamps. When either the K^+ or Ba^{++} concentration was changed, measurements were carried out after the current-voltage curve became steady; this usually took ~15 min. A triangular-shaped voltage command was used to monitor the current-voltage curve during the transient period. Experiments were carried out at 22–24°C.

2-2. Admittance Measurements and Model Curve Fit

Admittance determinations were made by a fast Fourier transform (FFT) calculation of current responses of the neuron to a Fourier synthesized pseudo random signal which was superposed as a small perturbation on a step voltage clamp (Fishman and Law, 1987). The synthesized signal was noise-like in that it contained 400 discrete frequency components, but deterministic in time because the digital values of the time series were stored in a read-only-memory device and, when desired, were outputed sequentially and periodically as an analog signal. The synthesized signal was applied to a computer through an anti-alias filter (elliptic 120 dB/oct) matched to the frequency band, and its real and imaginary parts, $V(j\omega)$, determined once by an FFT calculation and stored before acquisition of a response. The current response, $I(j\omega)$, of the neuron to the applied, synthesized voltage perturbations were acquired through the same anti-alias filter so that the filter's properties were eliminated from the driving-point admittance function ($Y[j\omega] = I[j\omega]/V[j\omega]$) determination. Real and imaginary parts of a current response were determined, and the admittance was computed using the previously stored real and imaginary parts of the synthesized voltage signal.

The spectral shape of the synthesized signal was made to approximate the inverse spectral property of the neuron responses. This results in a prewhitening of the responses, which significantly reduces errors due to the finite dynamic range of the digital signal processing section during

TABLE I
COMPOSITION OF EXTERNAL SOLUTIONS (MILLIMOLES/LITER)

	NaCl	Glucamine	KCl	$CaCl_2$	$MgCl_2$	$NiCl_2$	$BaCl_2$	Tris	pH
ASW	480	—	10	10	50 y	—	—	15	7.8
I	—	490-x	x	10	49 y	1	—	15	7.8
II	—	450	40	10	49-y	1	y	15	7.8

x = 0, 20, 40, and 100.
y = 0, 0.5, 1, and 5.

data acquisition and FFT calculation. Therefore, a complex admittance was rapidly determined with excellent resolution in any given frequency range. Averaging of the real and imaginary parts of several responses before computation of an admittance enabled enhancement of signal-to-noise ratio. The complex admittance was then stored as real and imaginary parts on a floppy disk for later retrieval and model curve fitting.

Admittances, determined with a very small amplitude (<0.5 mV) pseudorandom voltage signal, are noisy because of the introduction of significant sources of noise into the response from electrodes and instrumentation. With increases in pseudorandom stimulus intensity, an improved signal-to-noise ratio yields a virtually smooth admittance curve. With very large stimuli (>10 mV), an admittance determination again becomes noisy because the admittance reflects nonlinear responses to the stimulus (Fishman et al., 1981). In the case of *Aplysia* neurons with a diameter ~200 μm, 10 mV_{p-p} excursions of membrane potential yielded smooth admittance curves.

The magnitude spectrum obtained from the response of a 100 kΩ resistor to the synthesized signal was used for calibration of admittance magnitudes. The real and imaginary parts of the synthesized voltage signal were averaged 2 and 8 times and stored as a reference in the respective frequency ranges 0.05–20 Hz and 0.5–200 Hz. The real and imaginary parts of the neuronal membrane response were averaged 1 and 4 times in the respective frequency ranges 0.05–20 Hz and 0.5–200 Hz.

An LSI-11/73 central microprocessor and associated memory and peripheral devices (Digital Equipment Corp., Marlboro, MA) were used in the data acquisition and storage phase of the experiments. The microcomputer system was also used in conjuction with an array processor (SKY Computer Inc., Lowell, MA, SKYMNK-Q) for rapid computation and comparison of admittance models with admittance data. A curve fitting program using the method of least squares was used as described previously (Fishman et al., 1983). A model parameter was incremented or decremented until the chi-square statistic, used as a goodness-of-fit criterion for the fitting of admittance model functions to admittance data, did not improve. A single fitting run consisted of altering a model parameter separately from the others until a minimum chi-square value was obtained and then moving successively to each of the other parameters until alterations in all variable parameters had been tried. Many fitting runs (100) were required to obtain good fits and to approach a minimum chi-square value.

3. RESULTS

3-1. Current-Voltage Relationships

Fig. 2 *a* shows the dependence of the current-voltage relationship on external K^+ concentration. Inward current (negative sign) rectification is apparent at hyperpolarized potentials with increasing K^+ concentration. The conductance also increases with increased external K^+ concentration. The outward current, which appears in the depolarized potential region, is the delayed K^+ current. The curve observed in the K^+-free solution is not straight in the hyperpolarized potential region. Presumably, one of the reasons that inward K^+ current rectification still occurs in K^+-free media is due to residual K^+ that remains in the clefts of the membrane. Another possibility, which is considered subsequently, is that another rectifier channel, for example a Cl^- rectifier (Chenoy-Marchais, 1983), is activated.

Fig. 2 *b* shows the time dependence of the current-voltage curve in solution I without K^+. The curve is linear in the hyperpolarized potential region just after the electrodes were inserted into the cell. This indicates that, initially, there was no inward rectification. In other words, almost all of the K^+ close to the membrane or in the clefts was depleted by perfusing the neuron with K^+-free solution for more than 1 h. However, after the cell was clamped at hyperpolarized potential for ~20 min, the inward current increased despite the K^+-free condition. If the excess

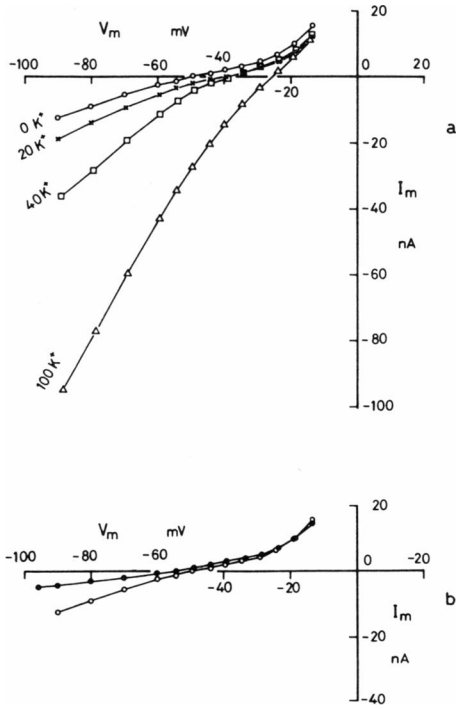

FIGURE 2 Current-voltage relationship of *Aplysia* neuron. Na^+ and Ca^{++} currents are suppressed in the Na^+-free medium with Ni^{++} ions. (*a*) The current-voltage curves at $[K^+]_o$ = 0, 20, 40, and 100 mM. (*b*) The current-voltage relationship observed at $[K^+]_o$ = 0 mM. ●; just after microelectrodes were inserted, and O; after the neuron was clamped at a hyperpolarized potential for ~20 min.

inward current results from residual K^+ in the clefts, the current-voltage curve should have shown an inward rectification just after the electrodes were inserted into the neuron. This time dependence of inward current rectification in K^+-free solution suggested that the nonlinear current-voltage relationship resulted from another inward rectification process that developed with time.

The Cl^- concentration in the cell is usually low. Therefore, the neuron does not show inward Cl^- current rectification (outwardly moving Cl^-) in the hyperpolarized potential region. Because 3 M KCl solution was used as the solution within the electrodes in these experiments, quite possibly Cl^- ions were injected into a neuron during measurements in which hyperpolarizing current flows through the intracellular electrode. Consequently, the neuron would show inward rectification of Cl^- current (Chenoy-Marchais, 1983), which would develop with time after electrode insertion.

3-2. Complex Admittance

Figs. 3 *a* and *b* show the dependence of the complex admittance on membrane potential in solution I with 40 and 0 mM K^+, respectively. The magnitude of the admittance observed at 40 mM K^+ concentration increases with hyperpolarization in the frequency range below 40 Hz. The admittance component above 40 Hz, which does not depend on membrane potential, is attributed to membrane capacitance. In contrast, the admittance observed in the K^+-free medium does not depend on membrane potential in the frequency range of 0.5–200 Hz. The dependence of the complex admittance on external K^+ concentration is also shown in Fig. 4 *a*. The admittance component below 40 Hz depends on K^+ concentration. This component is sensitive to both membrane potential and external K^+ concentration, which suggests that this component is associated with inward K^+ current rectification.

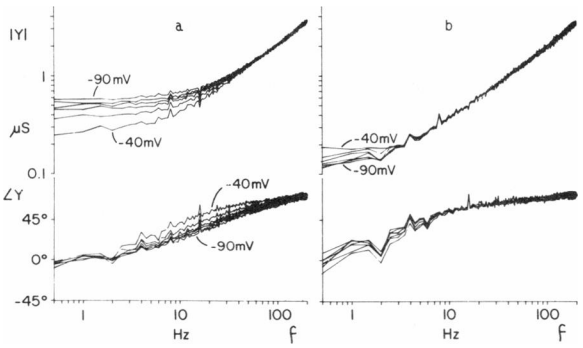

FIGURE 3 Dependence of the complex admittance on membrane potential. Na^+ and Ca^{++} conductions are suppressed in solution I. (*a*) The admittance determined at −40 to −90 mV, in 10 mV increments. External K^+ concentration is 40 mM. The magnitude of the admittance increases with hyperpolarization in the frequency range below 40 Hz. (*b*) The admittances as in *a* but in a solution without K^+ ions. The complex admittance in *b* does not depend on membrane potential because the inward K^+ current is suppressed.

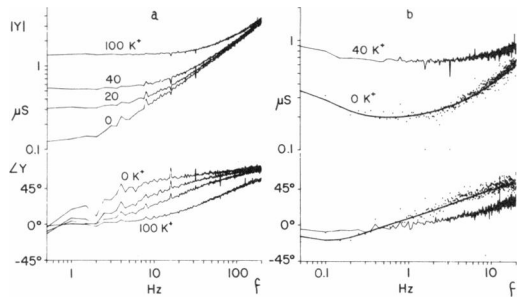

FIGURE 4 Dependence of the complex admittance on external K^+ concentration at a holding potential of −80 mV. (*a*) The admittance determined at $[K^+]_o$ = 0, 20, 40, and 100 mM in the frequency range 0.5–200 Hz. The magnitude of the admittance increases with increased K^+ concentration in the frequency range below 40 Hz. (*b*) The admittance determined at $[K^+]_o$ = 0 and 40 mM and at lower frequencies (0.05–20 Hz). The admittance shows that the low frequency inductive-like component (rise in the magnitude) reflects the kinetics of outwardly moving Cl^- ions.

Fig. 4 *b* shows the K^+ concentration dependence of the admittance at lower frequencies (0.05–20 Hz). The magnitude of the admittance component in the frequency range of 0.2–40 Hz, which is associated with rectification of inward K^+ current, decreases with a decrease in external K^+ concentration. The admittance has another inductive-like component on the low frequency side even in the K^+-free medium. The inductive-like component appears to correspond to rectification of inward Cl^- current because the characteristic frequency (below 0.1 Hz) agrees with that (0.02–0.3 Hz) obtained from the relaxation of voltage-clamp currents in *Aplysia* neuron by Chenoy-Marchais (1983).

The conductance (0.2 μS) of the inward K^+ rectifier at 1 Hz obtained from the magnitude of the admittance in Fig. 4 *b*, measured in K^+-free medium, agreed well with the conductance (0.13 μS) estimated from the linear portion of the current-voltage curve in Fig. 2 *b*, measured just after electrodes were inserted into the neuron. In addition, after the cell was clamped at a hyperpolarized potential for ~20 min, the conductance (0.35 μS) obtained from the admittance magnitude in Fig. 4 *b*, on the low frequency side in the K^+-free medium, agreed well with the conductance (0.35 μS) estimated from a linear slope approximation to the nonlinear current-voltage curve at potentials < -60 mV in Fig. 2 *b*. This suggests that the nonlinear current-voltage relation in the hyperpolarized region under the K^+-free condition is due to the rectification of inward Cl^- current.

3.3 Extraction of the Complex Conductance Associated with Inward K^+ Rectification from the Membrane Admittance

The rectification of inward K^+ current is quite large as shown in Fig. 2, and the complex admittance is sensitive to

membrane potential and K^+ concentration in the frequency range 0.2 to 40 Hz, as shown in Figs. 3 and 4. However, the magnitude of the admittance component associated with membrane capacitance is so large that the corner frequency of the admittance curve associated with the inward K^+ rectifier is obscured. For this purpose, it is necessary to extract the admittance component of the inward K^+ rectification process, i.e., the complex ionic conductance, from the total admittance which includes membrane capacitance.

An expression for the admittance of an axon membrane has been obtained by linearizing the Hodgkin-Huxley equations (Chandler et al., 1962). In our experiments, Na^+ and Ca^{++} currents of *Aplysia* neuron were suppressed in the Na^+-free medium with Ni^{++} ions. Inward membrane current of the neuron in the hyperpolarized potential region does not contain delayed outward K^+ current.

Therefore, the complex admittance of the neuron is;

$$Y(j\omega) = j\omega C_m + \{g_K + g_1/(1 + j\omega\tau_K)\} + \{g_{Cl} + g_2/(1 + j\omega\tau_{Cl})\} + g_L + Y_0(j\omega), \quad (1)$$

Where g_K and g_{Cl} are chord conductances of the K^+ and the Cl^- rectifiers, respectively and the complex conductance of the inward rectifier, $g(j\omega)$, is defined as

$$g(j\omega) = g'(\omega) + jg''(\omega) = g_K + g_1/(1 + j\omega\tau_K) + g_{Cl} + g_2/(1 + j\omega\tau_{Cl}). \quad (1a)$$

$g_1/(1 + j\omega\tau_K)$ and $g_2/(1 + j\omega\tau_{Cl})$ are frequency dependent conductances of each of the ionic rectifiers. It is assumed that the membrane capacitance, C_m, and the leakage conductance, g_L, are independent of membrane voltage and external K^+ concentration. The component Y_0 represents the admittance of the attached axon and the capacitance that results from the clefts of the neuron. The admittance that is expressed by Eq. 1 is realized with an electrical circuit as shown in Fig. 5 *a*. The circuit consists of parallel branches corresponding to each of the five terms in Eq. 1. The chord conductances of the K^+ and the Cl^- rectifier are grouped with the branches that correspond to each of the specific ion conduction processes. The admittance after suppression of both K^+ and Cl^- rectification processes, observed in the K^+-free medium and near resting potential, is

$$Y'(j\omega) = j\omega C_m + g_L + Y_0'(j\omega), \quad (2)$$

and the electrical circuit description is shown in Fig. 5 *b*. Then the complex subtraction of the admittance, Y', from the admittance Y, yields

$$Y - Y' = g_K + g_1/(1 + j\omega\tau_K) + g_{Cl} + g_2/(1 + j\omega\tau_{Cl}) + \Delta Y_0 = g(j\omega) + \Delta Y_0. \quad (3)$$

Where,

$$\Delta Y_0 = Y_0 - Y_0' \quad (4)$$

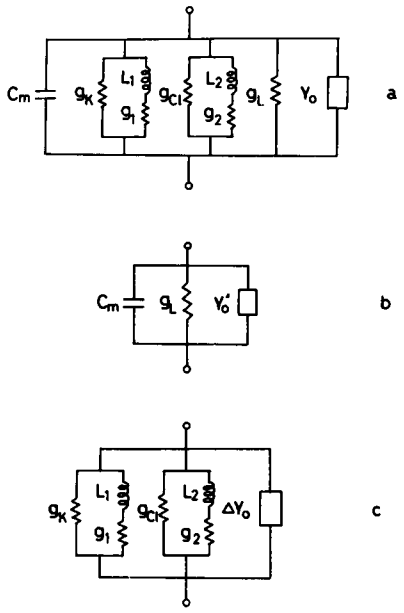

FIGURE 5 Linear electrical circuit description of membrane conduction from linearized, Hodgkin-Huxley type equations. (*a*) Circuit realization of the admittance, Y, in Eq. 1. The chord conductances of the K^+ and the Cl^- rectifiers are grouped with the branches corresponding to each of the specific ion conduction processes. (*b*) Circuit realization of the admittance, Y', in Eq. 2 when the K^+ and the Cl^- rectifiers are suppressed. (*c*) Electrical circuit obtained by subtraction of the admittance, Y', from the admittance, Y.

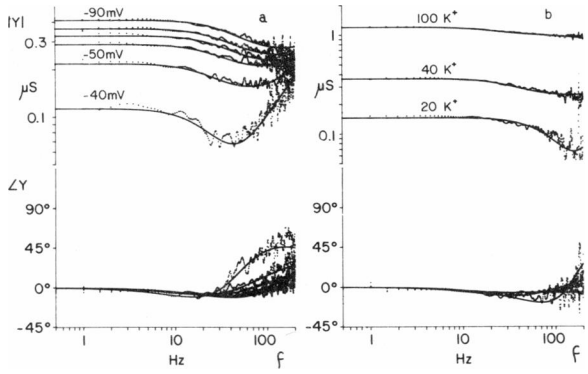

FIGURE 6 Complex admittance (conductance) separated from the membrane capacitance and the leakage conductance by complex vector subtraction (see text, Eq 3). The admittance reflects the inward K^+ rectification process and a high frequency capacitive-like component. The inductive-like component is due to the first-order kinetics of the inward K^+ rectifier. The capacitive-like component may be attributed to admittance changes in the attached axon or morphological changes in clefts which are induced by the external K^+ concentration change. The solid curves are the best fits to the data with the electrical circuit model in Fig. 7 *a*. (*a*) The extracted admittance in the potential range of -40 to -90 mV. External K^+ concentration is 40 mM. (*b*) The extracted admittance at $[K^+]_0$ = 20, 40, and 100 mM. Membrane potential is clamped at -80 mV.

and $g(j\omega)$ is the complex conductance of the inward rectifier. The electrical circuit description of the admittance is shown in Fig. 5 *c*. ΔY_0 results from the K^+-induced admittance changes in the attached axon or morphological changes of the clefts.

As mentioned above, rectification of inward K^+ current is adequately suppressed under K^+-free conditions. Rectification of inward Cl^- current increases with time in the hyperpolarized potential region. Therefore, the complex admittance observed in the K^+-free medium and near resting potential (−45 mV) is a good control for vector subtraction from the total admittance to obtain the complex conductance of the K^+ and Cl^- rectifiers. The admittances (complex conductances) obtained by vector subtraction were smoothed two times.

In Fig. 6 *a*, the admittances obtained by complex subtraction show inductive-like components corresponding to the inward K^+ rectifier. The magnitude of the admittance component in the frequency range below 40 Hz increases with hyperpolarization like the raw admittance in Fig. 3 *a*. The admittance still has a capacitive-like component above 40 Hz; the component appears near the resting potential, where the magnitude of the K^+ rectifier component is small. The capacitive-like component is not affected by membrane potential change. This component may correspond to K^+-induced admittance changes, ΔY_0, in the attached axon or morphological changes in clefts.

The admittance (complex conductance) component also depends on external K^+ concentration as shown in Fig. 6 *b*; the magnitude increases with an increased K^+ concentration.

3-4. Curve Fitting of the Complex Admittance with a Linearized Hodgkin-Huxley Type Model

The admittance obtained by complex subtraction in Fig. 6 consists of several components: the inward K^+ rectification, a residual capacitive component, and the frequency-independent component. Because, as mentioned in section 3-2, the characteristic frequency of the Cl^- rectifier is below 0.1 Hz, the Cl^- conductance contributes very little to the admittance in the frequency range 0.2–200 Hz. Thus the $L_2 - g_2$ branch in Fig. 5 *c* corresponding to Cl^- rectification is negligible. The steady-state conductance may contain a K^+-induced conductance change of axon channels. However, it may be assumed that the contribution to the conductance from axon channels is smaller than that of the inward K^+ rectifier channels. Therefore, the admittance change, ΔY_0, is approximately described by the $C_3 - g_3$ branch in Fig. 7 *a*. The circuit model shown in Fig. 7 *a* was used to simulate the admittance obtained by complex subtraction. The calculated admittance curves are shown by the solid lines in Fig. 6. The model gives excellent fits of the admittance data from which characteristic frequencies ranging from 19.9 to 38.8 Hz ($\tau_K = g_1 L_1 = 8$ to 4 ms) were obtained.

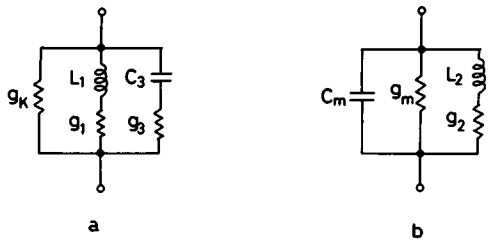

FIGURE 7 Electrical circuit model for curve fits. The circuit in *a* was used for curve fits to the complex conductances of the inward K^+ rectifier shown in Fig. 6. This circuit was also used for curve fits to the admittances in Fig. 12 which are affected by external Ba^{++}. The circuit in *b* was used for curve fits to the raw complex admittance data in Fig. 4 *b* which was observed at lower frequencies (0.05 to −20 Hz) in the K^+-free solution. $g_m = g_{Cl} + g_L$.

The raw complex admittance (0.05–20 Hz), shown in Fig. 4 *b*, observed at zero K^+ concentration and at −80 mV consists mainly of the Cl^- rectifier conductance, the membrane capacitance and the frequency independent leakage conductance. Therefore, the model in Fig. 7 *b* was used to simulate the low frequency admittance curve. g_m is the summation of the Cl^- and the leakage conductances; i.e., $g_m = g_{Cl} + g_L$. The $L_2 - g_2$ branch, corresponding to the kinetic process of the Cl^- channel, gives a relaxation time, $\tau_{Cl} = g_2 L_2$. The curve fits are also excellent as shown by the solid lines in Fig. 4 *b*; the characteristic frequency is 0.084 Hz (τ_{Cl} = 1.9 s). The ratio of the characteristic frequencies of the K^+ and the Cl^- rectifiers ranges from 273 to 462. Consequently, the admittance of the inward K^+ rectifier is easily distinguished in the frequency domain from the admittance of the Cl^- rectification process in *Aplysia* neuron.

3-5. Dependence of the Inward K^+ Rectifier Conductance and Relaxation Time on Membrane Potential

The total slope conductance which reflects K^+, Cl^-, and leakage conductances is obtained from a current-voltage relation in the hyperpolarized region. The closed circles in Fig. 8 *a* show the total conductance at 40 mM K^+ concentration. The magnitude of the plateau of the inductive-like component in Fig. 6 is the slope conductance of the inward K^+ rectifier. The values of the slope conductances are shown by the open circles in Fig. 8 *a*. Therefore, the difference between the total conductance curve (closed circles) and the *K* conductance curve (open circles) is the conductance curve of the Cl^- rectification process with leakage (*x*, symbols). the chord conductances of the inward K^+ rectifier, g_K, obtained by curve fits are also shown in Fig. 8 *a* by symbols, Δ.

The chord conductance of the inward K^+ rectifier increases and tends to saturate with hyperpolarization. The membrane potential dependence is similar to the dependence of the chord conductance of the inward K^+ rectifier observed in other cells (Marmor, 1971; Hagiwara and

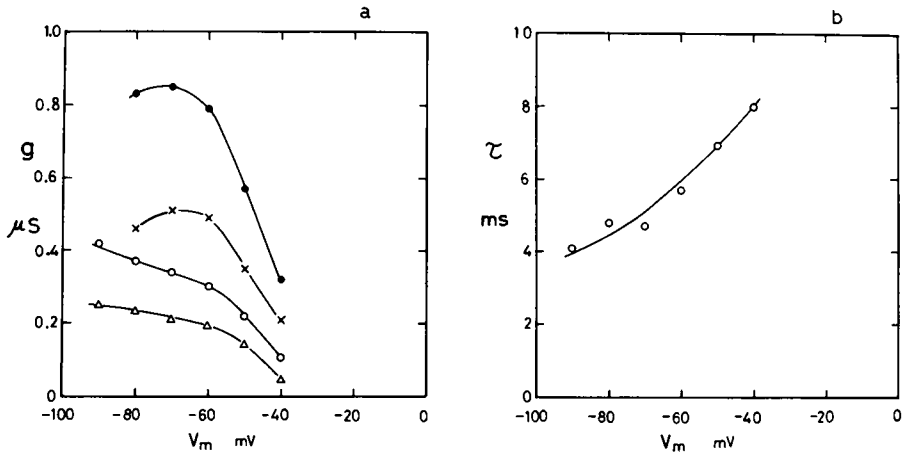

FIGURE 8 Dependence of the membrane conductance and the relaxation time on membrane potential. (*a*) External K^+ concentration is 40 mM. ●; total slope conductance obtained from the current-voltage curve, O; slope conductance obtained from the plateau of the admittance of the inward K^+ rectifier in Fig. 6 *a*, Δ; chord conductance of the inward K^+ rectifier obtained by curve fit of the admittance of the electrical circuit model in Fig. 7 *a* to the admittance in Fig. 6 *a* and x; Cl^- conductance obtained by subtraction of the inward K^+ rectifier slope conductance (O) from the total slope conductance (●). (*b*) Relaxation time of the inward K^+ rectifier process obtained by curve fits to the complex conductances in Fig. 6 *a*.

Takahashi, 1974) and muscle membranes (Leech and Stanfield, 1981; Hestrin, 1981). The slope conductance of the Cl^- rectifier shows an apparent hump in the region of −60 to −70 mV, although the Cl^- chord conductance that has been observed by Chenoy-Marchais (1983) exhibits a plateau. Thus the hump of the total slope conductance results from that of the Cl^- slope conductance.

Relaxation times of the inward K^+ rectifier are obtained by curve fit of the admittance of the electrical circuit model to the complex admittance data of the neuron. Fig. 8 *b* shows the membrane potential dependence of the relaxation time at 40 mM K^+ ion concentration. The relaxation time increases from 4 to 8 ms in the potential range of −90 to −40 mV.

3-6. Dependence of the Inward K^+ Rectifier Conductance and the Relaxation Time on External K^+ Ion Concentration

In the study of starfish egg cells the chord conductance of inward K^+ rectifier was determined to be proportional to the square root of external K^+ concentration (Hagiwara and Takahashi, 1974). The slope and chord conductances of the *Aplysia* neuron at −80 mV, which were obtained from the curve fits to the admittance component in Fig. 6 *b*, are shown in Fig. 9 *a*. The neuronal inward rectifier conductance also seems to be proportional to the square root of K^+ concentration. However, the straight line crosses the axis of $[K^+]_0^{1/2}$ at a positive value, which may indicate that this relationship is not valid at low $[K]_0$.

The relaxation time of the inward K^+ rectifier obtained by curve fit to the admittance component is shown in Fig. 9 *b* as a function of log $[K^+]_0$. The relaxation time increases monotonically with an increase in external K^+ concentration.

3-7. Effects of Ba^{++} on the Inward K^+ Rectification Process

Fig. 10 shows the dependence of the current-voltage relationship on Ba^{++} concentration. The inward current is reduced by increasing concentrations of Ba^{++}. The admit-

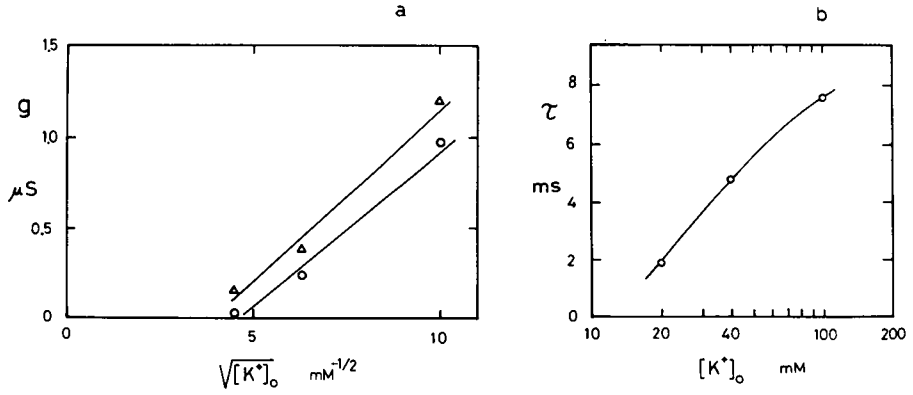

FIGURE 9 Dependence of the conductance and the relaxation time of the inward K^+ rectifier on external K^+ concentration. (*a*) The slope (Δ) and the chord (O) conductances. (*b*) the relaxation time. Membrane potential is clamped at −80 mV. These data were obtained by curve fits of the complex conductance of the electrical circuit model in Fig. 7 *a* to the complex conductances in Fig. 6 *b*.

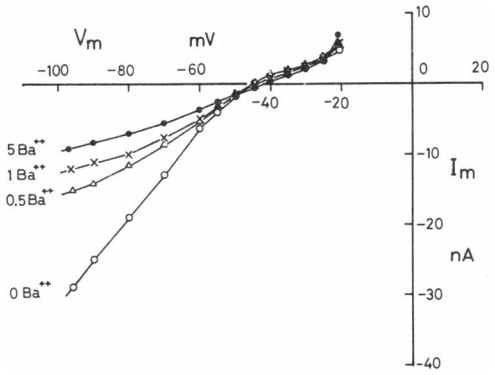

FIGURE 10 Current-voltage curves at $[Ba^{++}]_0$ = 0, 0.5, 1 and 5 mM. Na^+ and Ca^{++} conduction are suppressed in the Na^+-free medium with Ni^{++} ions. External K^+ concentration is 40 mM.

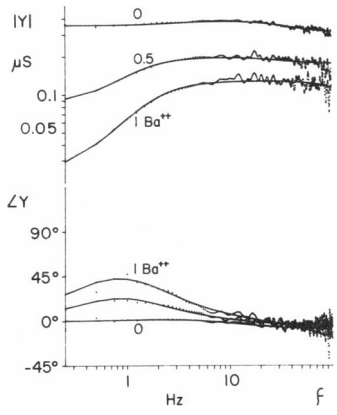

FIGURE 12 Complex conductances of the inward K^+ rectifier at $[Ba^{++}]_0$ = 0, 0.5, and 1 mM. The admittances of membrane capacitance and leakage conductance are removed by vector subtraction of a control admittance observed at $[Ba^{++}]_0$ = 5 mM and at −35 mV from the admittances observed at other Ba^{++} concentrations and at −80 mV. External K^+ concentration is 40 mM. S-shaped admittance magnitude reflects the first-order kinetics of the Ba^{++} blockade process. The solid lines are fitted curves with the complex conductance of the electrical circuit model shown in Fig. 7 *a*.

tance at a membrane potential of −80 mV is also affected by Ba^{++}, as shown in Fig. 11 *a*. The magnitude of the admittance in the frequency range below 40 Hz associated with the inward K^+ current rectification decreases with increases in Ba^{++} concentration. In contrast, the admittance at −35 mV is hardly affected by Ba^{++}, as shown in Fig. 11 *b*, because most of the inward K^+ rectifier channels are not activated at this membrane potential. Thus, the admittance at $[Ba^{++}]_0$ = 5 mM and at −35 mV is a good control for complex subtraction to unfold the admittance of all other conduction processes from the total admittance to obtain the admittance of the inward K^+ rectifier as it is affected by Ba^{++}.

Fig. 12 shows the admittance component of the inward K^+ rectifier at −80 mV that is partly blocked by Ba^{++}. The effect of Ba^{++} on the admittance is clearly different from that of external K^+. The decrease in the admittance magnitude on the low frequency side is larger than that on the high frequency side when external Ba^{++} concentration increases. In other words, a capacitive-like component appears in the admittance in the solution with Ba^{++}. The capacitive-like component is associated with the kinetics of Ba^{++} blockade of inward rectifier channels.

The admittance in Ba^{++} containing solutions shows two features: an inductive-like component corresponding to the inward K^+ rectifier itself and a capacitive-like component corresponding to the Ba^{++} blockade. Although another capacitive-like component that is associated with K^+-induced membrane admittance changes of attached axon or morphological change of the clefts may also exist, the admittance shows no capacitive-like component above 40 Hz. Therefore, a simple circuit model, similar to the one in Fig. 7 *a*, was used to simulate the admittance data. In this model, the c_3-g_3 branch and the L_1-g_1 branch are associated with the kinetic processes of Ba^{++} blockade and inward K^+ current rectification, respectively. The fitted curves, which are drawn solid lines, agree well with the admittance data, as shown in Fig. 12. Fig. 13 shows the relaxation time that is associated with the Ba^{++} blockade process as a function of log $[Ba^{++}]_0$. The relaxation time decreases with increases in Ba^{++} concentration.

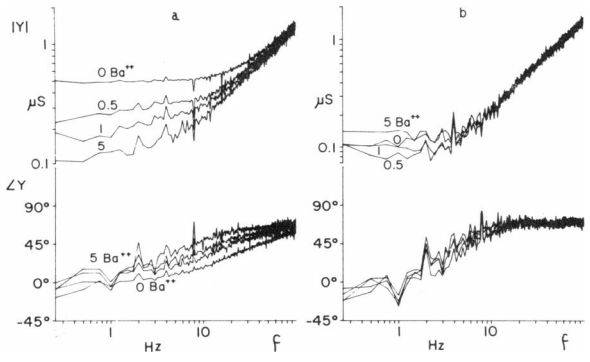

FIGURE 11 Complex admittance at $[Ba^{++}]_0$ = 0, 0.5, 1 and 5 mM. External K^+ is 40 mM. Membrane potentials is clampled at: (*a*) −80 and (*b*) −35 mV.

4. DISCUSSION

Here, we have assumed that the linearized properties of a single class of channels (inward K^+ rectifier) are reflected in the vector difference between the membrane admittance determined at zero-mean membrane current and at zero external K^+ concentration and the admittance determined at other membrane potentials and K^+ concentrations. The former admittance depends on membrane capacitance and all operative ion conductances (primarily leakage), whereas in the latter the inward rectifier conductance

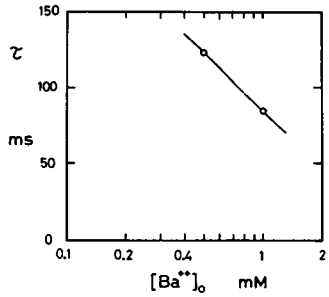

FIGURE 13 Relaxation time of the Ba^{++} blockade process of the inward K^+ rectifier obtained from the curve fits shown in Fig. 12. The solid line is the theoretical curve which was calculated with a two-conduction state model k_1 = 7,437 $s^{-1}M^{-1}$ and k_2 = 4.412 s^{-1}.

should dominate the total conductance. Furthermore, the above also assumes that leakage remains invariant with voltage and with changes in external K^+ concentrations. Assessment of the validity of these assumptions awaits measurement of the single-channel properties in this preparation. Nevertheless, the voltage- and K^+ concentration-dependence of inward rectifier conductance and kinetics and the description (that follows) of channel block by Ba^{++} reported here are in accordance with those described in other preparations, using methods other than admittance differences.

A mechanism for rectification in single-cardiac cells was recently suggested in two separate reports. In one (Matsuda et al., 1987) outward "whole-cell" current in inward rectifier, K^+ channels decayed with faster kinetics with increasing depolarizations from E_K, producing steady-state rectification in the current-voltage relation. Single channel recordings showed the channel conductance to be ohmic with diminishing times for channel closure with increasing depolarization, which accounts for the rectification observed as a reduced steady-state outward "whole-cell" current. These investigators also reported a blockade of inward rectifier, single K^+ channels by cytoplasmic-side Mg^{++}, producing an asymmetrical current-voltage relation at potentials depolarized from E_K. In the other report (Vandenberg, 1987) rectification of single channel current occurred only in the presence of Mg^{++} on the cytoplasmic side. Both studies used higher than normal physiological concentrations of K^+ during observation of Mg^{++} blockade. The results reported here cannot resolve these issues; however, the current-voltage relationship of Fig. 2 does not show the high rectification ratio (marked asymmetry) of cardiac cells and the relaxation time increases with depolarization (Fig. 8 *b*). Both of these characteristics suggest a nonohmic single channel conductance rather than rectification due to gating kinetics or a blocking ion.

The admittance component corresponding to the inward K^+ rectification process shows a first-order relaxation. A closed-open conduction state model,

$$C \underset{\beta(v)}{\overset{\alpha(v)}{\rightleftharpoons}} O, \tag{5}$$

was used to analyze the kinetic process of the inward K^+ rectifier. The dependence of the rate constants, α and β, on membrane potential are obtained from the dependence of the K^+ conductance, $g_K(v)$, and the relaxation time, $\tau_K(v)$, on membrane potential:

$$\alpha(v) = [g_K(v)/g_{max}][1/\tau_K(v)]. \tag{6}$$

$$\beta(v) = [1 - (g_K(v)/g_{max})][1/\tau_K(v)]. \tag{7}$$

Where, g_{max} is the steady state maximum conductance. Fig. 14 shows the membrane potential dependence of the rate constants which were calculated using the chord conductance in Fig. 8 *a* and the relaxation time in Fig. 8 *b*.

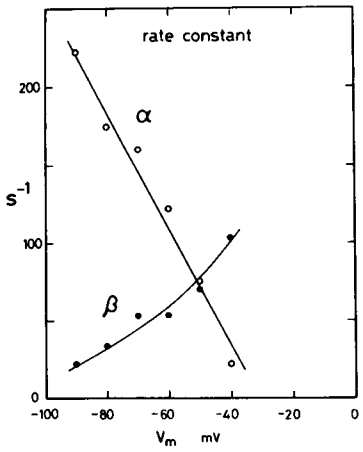

FIGURE 14 Membrane potential dependence of the rate constants. A two-conduction state model was applied to the inward K^+ rectification process observed in the solution with 40 mM K^+. g_{max} = 0.28 μs.

The forward rate constant, α, increases and backward rate constant, β, decreases with hyperpolarization.

The admittance (complex conductance) in the solution with Ba^{++}, which was obtained by subtraction, contains mainly a capacitive-like component that reflects the Ba^{++} blockade of the channel and an inductive-like component that is associated with the inward K^+ rectifier itself. On the basis of the two-conduction state model, a three-state model,

$$C \underset{\beta}{\overset{\alpha}{\rightleftharpoons}} O \underset{k_2}{\overset{k_1}{\rightleftharpoons}} B, \tag{8}$$

was applied to explain the Ba^{++} blockade of the inward K^+ rectifier channel. "*B*" is the state of Ba^{++} blockade of the channel. Although transitions between closed and blocked states may occur, this type of transition is neglected here for simplicity. The rate constants, α and β, depend not only on membrane potential but also on K^+ ion concentration. The rate constants, k_1 and k_2, depend only on membrane potential here following the theory of Warncke and Lindemann (1985). Because the ratio of the characteristic frequencies of the inward K^+ rectifier and the Ba^{++} blockade processes is more than 20, each of the kinetic processes $C \rightleftharpoons O$ and $O \rightleftharpoons B$ is considered independently, even though they coexist.

First, the left part of state diagram (8),

$$C \underset{\beta}{\overset{\alpha}{\rightleftharpoons}} O, \tag{9}$$

is considered. The rate equation is

$$dP/dt = \alpha(v, C_K)(1 - P) - \beta(v, C_K)P. \tag{10}$$

P denotes the probability that the channel is conducting. C_K and v are K^+ concentration and potential difference across the membrane, respectively. Following the procedure of Warncke and Lindemann (1985), the complex conductance (admittance) and magnitude are as follows;

$$Y = G_1 + \frac{\Delta G}{1 + (\omega\tau)^2} - j\frac{\Delta G\omega\tau}{1 + (\omega\tau)^2} \tag{11}$$

and

$$|Y| = \frac{\{[G_1 + \Delta G + G_1(\omega\tau)^2]^2 + [(\Delta G\omega\tau)^2]\}^{1/2}}{1 + (\omega\tau)^2} \quad (12)$$

Where,

$$\Delta G = I_K\tau[(\beta/\alpha)(d\alpha/dv) - d\beta/dv] \quad (13)$$

$$\tau = (\alpha + \beta)^{-1}, \quad (14)$$

and

$$G_1 = (\alpha\tau)(dI_0/dv) \quad (15)$$

I_K is K^+ current and I_0 is the maximum K^+ current when external K^+ concentration is sufficiently high. In Eq. 12, if $\Delta G > 0$, the admittance is inductive, and if $\Delta G < 0$, the admittance is capacitive.

The rate constant, α, increases and the rate constant, β, decreases with hyperpolarization as shown in Fig. 14. Then $\Delta G > 0$ because $d\alpha/dv > 0$, $d\beta/dv < 0$, $I_K > 0$, and $(\beta/\alpha) > 0$. Thus, the complex conductance that is associated with the inward K^+ rectifier kinetics has an imaginary part that is inductive.

Next, the other part of the reaction,

$$O \underset{k_2}{\overset{k_1}{\rightleftharpoons}} B, \quad (16)$$

is considered. The rate equation is

$$dP/dt = k_2(v)(1 - P) - k_1(v)\,C_{Ba}P. \quad (17)$$

P in this equation is the probability that a channel is not blocked by Ba^{++}. C_{Ba} is Ba^{++} concentration. The complex admittance and its magnitude reduced from Eq. 17 are the same formalism as Eqs. 11 and 12 except that

$$\Delta G = I_K C_{Ba}\,[(k_1/k_2)\,(dk_2/dv) - dk_1/dv] \quad (18)$$

$$\tau(v) = [k_1(v)\,C_{Ba} + k_2(v)]^{-1} \quad (19)$$

and

$$G_1 = (k_2\tau)\,(dI_0/dv). \quad (20)$$

The membrane potential dependence of the rate constants, k_1 and k_2, which are associated with the blockade kinetics, have been determined by Eaton, Brodwick and Ifshin (personal communication); the rate constant, k_1, increases with hyperpolarization and the rate constant, k_2, does not depend on the membrane potential. Because $I_K > 0$, $dk_1/dv > 0$, and $dk_2/dv = 0$, ΔG is negative. This indicates that the complex conductance that is associated with the kinetics of Ba^{++} blockade has an imaginary part that is capacitive.

The Ba^{++} concentration dependence of the relaxation time, τ_{Ba}, which was calculated by Eq. 19 with $k_1 = 7{,}437$ $s^{-1}M^{-1}$ and $k_2 = 4.412\ s^{-1}$ is consistent with the relaxation time which is observed in *Aplysia* neurons as shown in Fig. 13.

Warncke-Lindemann analysis (1985) is based on a plug-type blocking model which has been proposed by Cuthbert (1976); a positive charged part of the molecule occupies the channel entrance during blockade. The Ba^{++} blockade of the inward K^+ rectifier is explained qualitatively by their analysis based on a two-state model. Therefore, a first-order blocking model is compatible with the kinetics of Ba^{++} blockade. The simplest interpretation of the first-order blocking kinetics is that Ba^{++} binds to an entrance site of the inward K^+ rectifier thereby occluding the channel.

The authors are grateful to Dr. J. Blankenship for instruction on the dissection of *Aplysia*. We also thank Dr. D. C. Eaton for helpful discussion of blockers of the inward K^+ rectification channel and Dr. J. M. Russell for advice on media for *Aplysia* neurons and enzymes to soften the connective tissue capsule. Mr. William Law, Jr. designed the voltage clamp circuit and produced the software for data acquisition and analysis. Ms. Catheryne Randall typed the manuscript.

Supported in part by National Institutes of Health grant NS13778 and by contract N00014-87-K-0055 from the Office of Naval Research.

Received for publication 12 August 1987 and in final form 17 December 1987.

REFERENCES

Adrian, R. H., and W. H. Freygang. 1962. The potassium and chloride conductance of frog muscle membrane. *J. Physiol.* (*Lond.*). 163:61–103.

Adrian, R. H., W. K. Chandler, and A. L. Hodgkin. 1970. Slow changes in potassium permeability in skeletal muscle. *J. Physiol.* (*Lond.*). 208:645–668.

Brodwick, M. S., and D. Junge. 1972. Post-stimulus hyperpolarization and slow potassium conductance increase in *Aplysia* giant neurone. *J. Physiol.* (*Lond.*). 223:549–570.

Chandler, W. K., R. FitzHugh, and K. S. Cole. 1962. Theoretical stability properties of a space-clamped axon. *Biophys. J.* 2:105–127.

Chenoy-Marchais, D. 1983. Characterization of a chloride conductance activated by hyperpolarization in *Aplysia* neurons. *J. Physiol.* (*Lond.*). 342:277–308.

Cuthbert, A. W. 1976. Importance of guanidinium groups for blocking sodium channels in epithelia. *Mol. Pharmacol.* 12:945–957.

Eckert, R., and H. D. Lux. 1976. A voltage-sensitive persistent calcium conductance in neuronal somata of *Helix*. *J. Physiol.* (*Lond.*). 254:129–151.

Fishman, H. M., and W. C. Law, Jr. 1987. Rapid acquisition and analysis of driving-point functions in nerve membranes. Proc. 9th Ann. Conf. IEEE (Inst. Electr. Electron. Eng.) Engineering in Medicine and Biology Society vol 2.

Fishman, H. M., L. E. Moore, and D. Poussart. 1981. Squid axon K conduction: admittance and noise during short- versus long-duration step clamps. *In* The Biophysical Approach to Excitable Systems. W. J. Adelman and D. E. Goldman, editors. Plenum Publishing Co., New York. pp. 65–95.

Fishman, H. M., H. R. Leuchtag, and L. E. Moore. 1983. Fluctuation and linear analysis of Na-current kinetics in squid axon. *Biophys. J.* 43:293–307.

Gallin, K. E. 1981. Voltage clamp studies in macrophages from mouse spleen cultures. *Science* (*Wash., DC*). 214:458–460.

Geduldig, D. and R. Gruener. 1970. Voltage clamp of the *Aplysia* giant neurone: early sodium and calcium current. *J. Physiol.* (*Lond.*). 211:217–244.

Gunning, R. 1983. Kinetics of inward rectifier gating in the eggs of the

marine polychaete, *Neanthes arenaceodentata*. *J. Physiol.* (*Lond.*). 342:437–451.

Gunning, R. 1984. Steady-state current noise from the intrinsic gating of inward rectifier channels. *Biophys. J.* 45:1031–1035.

Hagiwara, S., K. Kusano, and N. Saito. 1961. Membrane changes of *Onchidium* nerve cell in potassium-rich media. *J. Physiol.* (*Lond.*). 155:470–489.

Hagiwara, S., and K. Takahashi. 1974. The anomalous rectification and cation selectivity of the membrane of a starfish egg cell. *J. Membr. Biol.* 18:61–80.

Hayashi, H., and H. M. Fishman. 1986. The complex conductance of the inward K current rectification process in *Aplysia* neurons. *Biophys. J.* 49:165. (Abstr.)

Hestrin, S. 1981. The interaction of potassium with the activation of anomalous rectification in frog muscle membrane. *J. Physiol.* (*Lond.*). 317:497–508.

Hutter, O. F., and D. Noble. 1960. Rectifying properties of heart muscle. *Nature* (*Lond.*). 188:495.

Kandel, E. R., and L. Tauc. 1964. An anomalous form of rectification in a molluscan central neurone. *Nature* (*Lond.*). 202:1339–1341.

Kandel, E. R., and L. Tauc. 1966. Anomalous rectification in the metacerebral giant cells and its consequences for synaptic transmission. *J. Physiol.* (*Lond.*). 183:287–304.

Katz, B. 1949. Les constantes electriques de la membrane du muscle. *Arch. Sci. Physiol.* 3:285–300.

Leech, C. A., and P. R. Stanfield. 1981. Inward rectification in frog skeletal muscle fibres and its dependence on membrane potential and external potassium. *J. Physiol.* (*Lond.*). 319:295–309.

Marmor, M. F. 1971. The effects of temperature and ions on the current–voltage relation and electrical characteristics of a molluscan neurone. *J. Physiol.* (*Lond.*). 218:573–598.

Matsuda, H., A. Saigusa, and H. Irisawa. 1987. Ohmic conductance through the inwardly rectifying K channel and blocking by internal Mg^{++}. *Nature* (*Lond.*). 325:156–159.

Meech, R. W., and N. B. Standen. 1975. Potassium activation in *Helix aspersa* neurons under voltage clamp: a component mediated calcium influx. *J. Physiol.* (*Lond.*). 249:211–239.

Miyamoto, S., and H. M. Fishman. 1986. Na conductance kinetics in the low frequency impedance of isolated snail neurons. *IEEE* (*Inst. Electr. Electron. Eng.*) *Trans. Biomed. Eng.* 33:644–653.

Nakajima, S., S. Iwasaki, and K. Obata. 1962. Delayed rectification and anomalous rectification in frog's skeletal muscle membrane. *J. Gen. Physiol.* 46:97–115.

Nelson, P. G., and K. Frank. 1967. Anomalous rectification in the meta cerebral giant cells and its consequences for synaptic transmission. *J. Physiol.* (*Lond.*). 183:287–304.

Noble, D. 1979. The Initiation of the Heart Beat. Clarendon, Oxford. 186 pp

Ohmori, H. 1980. Dual effects of K ions upon the inactivation of the anomalous rectifier of the tunicate egg cell membrane. *J. Membr. Biol.* 53:143–156.

Reuben, J. P., and H. Gainer. 1962. Membrane conductance during depolarizing postsynaptic potentials of crayfish muscle fibres. *Nature* (*Lond.*). 193:142–143.

Vandenberg, C. 1987. Inward rectification of a potassium channel in cardiac ventricular cells depends on internal magnesium ions. *Proc. Natl. Acad. Sci. USA.* 84:2560–2564.

Warncke, J., and B. Lindemann. 1985. Voltage dependence of Na channel blockage by Amiloride: relaxation effects in admittance spectra. *J. Membr. Biol.* 86:255–265.

Werblin, F. S. 1979. Time- and voltage-dependent ionic components of the rod response. *J. Physiol.* (*Lond.*). 294:613–626.